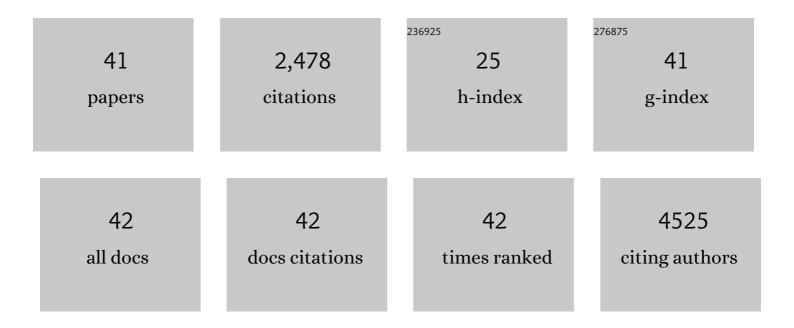
Berend T Jonker

List of Publications by Year in descending order

Source: https://exaly.com/author-pdf/1828854/publications.pdf Version: 2024-02-01



#	Article	IF	CITATIONS
1	Laser-Patterned Submicrometer Bi ₂ Se ₃ –WS ₂ Pixels with Tunable Circular Polarization at Room Temperature. ACS Applied Materials & Interfaces, 2022, 14, 9504-9514.	8.0	2
2	Visualizing band structure hybridization and superlattice effects in twisted MoS ₂ /WS ₂ heterobilayers. 2D Materials, 2022, 9, 015032.	4.4	9
3	Nanoscale Optical Imaging of 2D Semiconductor Stacking Orders by Excitonâ€Enhanced Second Harmonic Generation. Advanced Optical Materials, 2022, 10, .	7.3	9
4	Spin-Sensitive Epitaxial In ₂ Se ₃ Tunnel Barrier in In ₂ Se ₃ /Bi ₂ Se ₃ Topological van der Waals Heterostructure. ACS Applied Materials & Interfaces, 2022, 14, 34093-34100.	8.0	2
5	Direct-Write of Nanoscale Domains with Tunable Metamagnetic Order in FeRh Thin Films. ACS Applied Materials & Interfaces, 2021, 13, 836-847.	8.0	21
6	Probing Electronic Structures of Monolayer WSe2 Stacked with hBN Using Correlative Cathodoluminescence and Electron Energy-Loss Spectroscopy. Microscopy and Microanalysis, 2021, 27, 1174-1176.	0.4	1
7	Stacking-dependent optical properties in bilayer WSe ₂ . Nanoscale, 2021, 14, 147-156.	5.6	16
8	Continuous Wave Sum Frequency Generation and Imaging of Monolayer and Heterobilayer Two-Dimensional Semiconductors. ACS Nano, 2020, 14, 708-714.	14.6	41
9	Twist Angle-Dependent Atomic Reconstruction and Moiré Patterns in Transition Metal Dichalcogenide Heterostructures. ACS Nano, 2020, 14, 4550-4558.	14.6	172
10	Direct observation of minibands in a twisted graphene/WS ₂ bilayer. Science Advances, 2020, 6, eaay6104.	10.3	39
11	Emergent electric field control of phase transformation in oxide superlattices. Nature Communications, 2020, 11, 902.	12.8	35
12	Synthesis of High-Quality Monolayer MoS ₂ by Direct Liquid Injection. ACS Applied Materials & Interfaces, 2020, 12, 9580-9588.	8.0	9
13	Chemical Identification of Interlayer Contaminants within van der Waals Heterostructures. ACS Applied Materials & Interfaces, 2019, 11, 25578-25585.	8.0	43
14	Efficient spin current generation in low-damping Mg(Al, Fe)2O4 thin films. Applied Physics Letters, 2019, 115, .	3.3	21
15	Imaging microscopic electronic contrasts at the interface of single-layer WS2 with oxide and boron nitride substrates. Applied Physics Letters, 2019, 114, 151601.	3.3	14
16	Spatially Selective Enhancement of Photoluminescence in MoS ₂ by Exciton-Mediated Adsorption and Defect Passivation. ACS Applied Materials & Interfaces, 2019, 11, 16147-16155.	8.0	47
17	Ultrafast Carrier Dynamics of Monolayer WS ₂ via Broad-Band Time-Resolved Terahertz Spectroscopy. Journal of Physical Chemistry C, 2019, 123, 30676-30683.	3.1	12
18	Resonant optical Stark effect in monolayer WS2. Nature Communications, 2019, 10, 5539.	12.8	46

Berend T Jonker

#	Article	IF	CITATIONS
19	Quantum Calligraphy: Writing Single-Photon Emitters in a Two-Dimensional Materials Platform. ACS Nano, 2019, 13, 904-912.	14.6	80
20	Nano-"Squeegee―for the Creation of Clean 2D Material Interfaces. ACS Applied Materials & Interfaces, 2018, 10, 10379-10387.	8.0	124
21	Giant spin-splitting and gap renormalization driven by trions in single-layer WS2/h-BN heterostructures. Nature Physics, 2018, 14, 355-359.	16.7	83
22	Electrical Characterization of Discrete Defects and Impact of Defect Density on Photoluminescence in Monolayer WS ₂ . ACS Nano, 2018, 12, 1793-1800.	14.6	106
23	Double Indirect Interlayer Exciton in a MoSe ₂ /WSe ₂ van der Waals Heterostructure. ACS Nano, 2018, 12, 4719-4726.	14.6	160
24	A- and B-exciton photoluminescence intensity ratio as a measure of sample quality for transition metal dichalcogenide monolayers. APL Materials, 2018, 6, .	5.1	103
25	Understanding Variations in Circularly Polarized Photoluminescence in Monolayer Transition Metal Dichalcogenides. ACS Nano, 2017, 11, 7988-7994.	14.6	56
26	Photoinduced Bandgap Renormalization and Exciton Binding Energy Reduction in WS ₂ . ACS Nano, 2017, 11, 12601-12608.	14.6	112
27	Homoepitaxial graphene tunnel barriers for spin transport. AIP Advances, 2016, 6, .	1.3	7
28	Graphene and monolayer transition-metal dichalcogenides: properties and devices. Journal of Materials Research, 2016, 31, 845-877.	2.6	15
29	Spatial Control of Photoluminescence at Room Temperature by Ferroelectric Domains in Monolayer WS ₂ /PZT Hybrid Structures. ACS Omega, 2016, 1, 1075-1080.	3.5	25
30	Auger Recombination in Chemical Vapor Deposition-Grown Monolayer WS ₂ . Journal of Physical Chemistry Letters, 2016, 7, 5242-5246.	4.6	85
31	The Effect of Preparation Conditions on Raman and Photoluminescence of Monolayer WS2. Scientific Reports, 2016, 6, 35154.	3.3	107
32	Synthesis of Large-Area WS2 monolayers with Exceptional Photoluminescence. Scientific Reports, 2016, 6, 19159.	3.3	153
33	Spatially Resolved Electronic Properties of Single-Layer WS ₂ on Transition Metal Oxides. ACS Nano, 2016, 10, 10058-10067.	14.6	31
34	Exciton diamagnetic shifts and valley Zeeman effects in monolayer WS2 and MoS2 to 65 Tesla. Nature Communications, 2016, 7, 10643.	12.8	253
35	Charge Trapping and Exciton Dynamics in Large-Area CVD Grown MoS ₂ . Journal of Physical Chemistry C, 2016, 120, 5819-5826.	3.1	111
36	Hydrogenated Graphene as a Homoepitaxial Tunnel Barrier for Spin and Charge Transport in Graphene. ACS Nano, 2015, 9, 6747-6755.	14.6	36

3

Berend T Jonker

#	Article	IF	CITATIONS
37	Spin Coherence and Dephasing of Localized Electrons in Monolayer MoS ₂ . Nano Letters, 2015, 15, 8250-8254.	9.1	49
38	Homoepitaxial tunnel barriers with functionalized graphene-on-graphene for charge and spin transport. Nature Communications, 2014, 5, 3161.	12.8	67
39	Largeâ€Area Synthesis of Continuous and Uniform MoS ₂ Monolayer Films on Graphene. Advanced Functional Materials, 2014, 24, 6449-6454.	14.9	149
40	Control of magnetic contrast with nonlinear magneto-plasmonics. Scientific Reports, 2014, 4, 6191.	3.3	19
41	Direct-Write of Nanoscale Domains with Tunable Metamagnetic Order in FeRh Thin Films. , 0, .		1